Journal of Imaging Science and Technology® 56(4): 040504-1–040504-5, 2012.

Inkjet Printing Technology for OPV Applications

Maosheng Ren[†], **Jörgen Sweelssen, Nadia Grossiord, Harrie Gorter, Tamara Marijke Eggenhuisen, and Ronn Andriessen**[†]
Holst Centre/TNO, High Tech Campus 31, 5605 KN Eindhoven, the Netherlands
E-mail: mren538@gmail.com

Abstract. *Large-scale production of organic photovoltaics (OPVs) at low cost is, still, a future concept thought to promote the market share of solar energy. Working towards the roll-to-roll production of OPVs, different compatible deposition techniques are investigated. Inkjet printing is a promising candidate, as it allows the contact-free deposition of patterned functional materials with high flexibility. In this article, we further extend the application of inkjet printing for roll-to-roll production of OPVs. Inkjet-printed high-conducting PEDOT:PSS is compatible with indium tin oxide-free devices, by combination with an Ag grid to form the anode. A P3HT/PCBM layer is inkjet printed on top using non-chlorinated halogen-free solvents only, and large-area homogeneous layers with surface areas up to 3 cm by 3 cm were obtained. The device thus manufactured showed performance comparable to a reference device with spin-coated layers for which chlorobenzene was used as solvent for the photoactive layer. This is an essential step forward in the knowledge on materials and process conditions using inkjet printing for OPVs and working towards the full roll-to-roll production of OPVs without loss of performance.* *© 2012 Society for Imaging Science and Technology.*

[DOI: 10.2352/J.ImagingSci.Technol.2012.56.4.040504]

INTRODUCTION

Organic photovoltaics (OPVs) currently only present a minority share of the solar energy market. Nevertheless, they are considered to have large share potential, due to the promise of low-cost manufacturing by roll-to-roll technology.[1–3] However, up to now their break-through has been hampered by some fundamental and technological challenges. Their stability and life time as well as low conversion efficiency need to be increased before they can enter the solar energy market. In addition, to exploit the potential of roll-to-roll production, the solution processing of all the layers that assemble an OPV device needs to be developed. Several groups have reported functioning OPV modules manufactured by a roll-to-roll process, mainly using slot-die coating.[4,5]

Inkjet printing is a promising candidate among the techniques compatible with roll-to-roll production.[6,7] It is a contact-free deposition method that offers flexibility in terms of patterning as well as the functional material that is being deposited. Indeed, inkjet printing of one or several layers of the OPV has been reported.[8,9] In this article we describe another step forward in the application of inkjet printing for roll-to-roll processing by addressing two major challenges: using indium tin oxide-free electrodes and stepping away from chlorinated solvents for the photoactive layer.

Indium tin oxide (ITO) has long been the best transparent electrode, and it has been applied for many a device. However, to obtain its low sheet resistivity of 5–15 $\Omega/\square$, a thermal annealing step is applied, improving the crystallinity of the material. This is not freely compatible with roll-to-roll systems using polymer foils as substrate. Patterned ITO on flexible foils have been demonstrated with sheet resistivity in the order of 30–60 $\Omega/\square$.[10] Furthermore, the limited resources of indium provide further motivation to replace the transparent electrode with a less expensive, more abundant material. Working towards a solution, an electrode of a Ag grid combined with high-conducting PEDOT:PSS has been developed with sheet resistivity down to 5 $\Omega/\square$.[11,12]

The photoactive layer forms the heart of the OPV, and its structure is determinant for the performance of the device. The morphology of the donor and acceptor domains in bulk heterojunction (BHJ) cells depends on the solvent used, the drying and annealing procedure, and the donor/acceptor phase behavior.[13] For most BHJ systems, the performance of solution-processed cells has been optimized using chlorinated aromatic solvents, due to the good solubility of most donor polymers and acceptors. For P3HT/PCBM, a commercially available donor/acceptor bulk heterojunction system, processing by inkjet printing using chlorobenzene or dichlorobenzene has been reported.[14–16] However, expelling the use of environmentally hazardous and health-risking solvents is highly desirable, if not a prerequisite, for large-scale production. Finding an alternative solvent is complicated due to the delicate balance between many requirements. First, the donor and acceptor have to be soluble, preferably up to 2 wt% of each component, without aggregation or gelation over time. Then, to yield an inkjet-printable ink, there are limits in terms of viscosity, surface tension, and boiling points. The wetting of the substrate by the ink should lead to a homogeneous spreading and uniform layer formation. Finally, and possibly most importantly, the bulk heterojunction morphology in the deposited layer needs to be optimal to yield a good device performance.

Inkjet printing the transparent electrode and using non-chlorinated solvents for the photoactive layer are important steps towards the realization of a roll-to-roll process manufacturing OPV devices, as laid out in Figure 1.

[†] Present address: Mutracx B.V., Lagedijk 32, Helmond, the Netherlands.

Received Mar. 30, 2012; accepted for publication Sep. 19, 2012; published online Dec. 6, 2012.
1062-3701/2012/56(4)/040504/05/$20.00

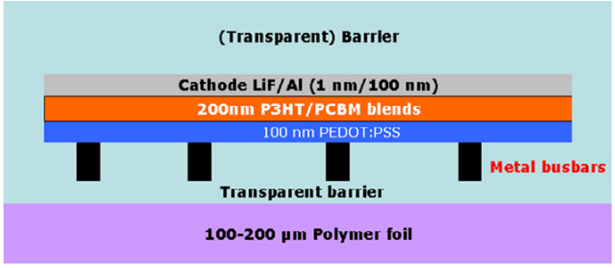

Figure 1. Schematic drawing of an ITO-free OPV stack on foil.

EXPERIMENTAL METHODS

Materials

High-conducting poly(3,4-ethylenedioxythiophene):poly-(styrenesulfonate) (PEDOT:PSS, 1% in water) was obtained from Agfa (Orgacon™ HIL1005 IJ, Agfa-Gevaert N.V.), poly-(3-hexylthiophene) (P3HT) was purchased from both Merck (Lisicon SP001) and Plextronics (Plexcore OS 2100), and (6,6)-phenyl C61-butyric acid methylester (PCBM, 99%) from Solenne BV. Solvents were obtained from Sigma-Aldrich and used as received.

Inkjet printing

Deposition of the PEDOT:PSS layer was carried out using a piezoelectrically actuated Spectra Galaxy PH 256/50 AAA inkjet printer head. The nozzle pitch was 254 µm, while the drop volume and drop ejection frequency were kept constant at 50 pL and 1 kHz, respectively. The lateral separation of neighboring printed lines was varied by adjusting the azimuthal orientation of the printer head with respect to the direction of substrate motion. To test the wetting of high-conducting PEDOT:PSS on SiN_x and Ag, a test pattern of Ag lines was printed onto a glass/SiN_x substrate, where the SiN_x was applied by chemical vapor deposition. The silver lines were printed using Cabot AG-IJ-G-100-S1 silver nanoparticle ink. The pattern was deposited using a Fujifilm Dimatix Materials printer (DMP 2831) with a 16 nozzle print head.

For the P3HT/PCBM layer, P3HT and PCBM were dissolved in non-chlorinated solvents in a 1:1 ratio by weight and at a total solids concentration of 2–4 wt%. To dissolve the polymer and PCBM, the solutions were stirred for 14 h at 70°C under ambient conditions. The ink was subsequently cooled down to room temperature and processed within 30 min to prevent gelation. Inkjet printing was performed on a FujiFilm Dimatix Materials Printer (DMP 2831) with a 16 nozzle print head. The drop spacing was set to 30 µm and the drop volume was 10 pL.

Device stack

OPV devices were fabricated on 3 cm by 3 cm glass substrates patterned with ITO. The substrates were cleaned by washing with Teepol/water and ultrasonication in acetone and isopropanol. Prior to deposition of PEDOT:PSS, the substrates were treated with UV/O_3 for 10 min. High-conducting PEDOT:PSS was deposited by inkjet printing (as described above) and dried at 130°C. Subsequently, P3HT/PCBM (0.8 wt%/0.8 wt%) was inkjet printed and annealed at 130°C. The nominal layer thicknesses of the dried PEDOT:PSS and P3HT/PCBM layers were 100 and 300 nm, respectively. Finally, the metal cathode (1 nm LiF, 100 nm Al) was thermally evaporated in a vacuum chamber through a shadow mask. As a reference, a fully spin-coated device was produced by spin coating PEDOT:PSS and P3HT/PCBM (2 wt%/2 wt% in chlorobenzene) with dried layer thicknesses of 100 and 300 nm, respectively.

Characterization

The current density–voltage (I–V) characteristics of the OPV devices were measured using a xenon lamp, which was calibrated with a standard silicon photodiode detector. The active area of the devices varied between 2 mm by 2 mm and 10 mm by 10 mm. The light source was a Xenon-lamp solar simulator, which was calibrated with a standard silicon photodiode detector. Life time tests were done by measuring the performance of the devices over time. The life time conditions for the samples were the following: dark at room temperature, dark at 45°C and illuminated using a G2 light engine combined with a S-bulb (Solaronix), at 1 sun, at 45°C. Viscosity measurements of inks were performed after heating the inks at 70°C and cooling to 20°C using the rolling ball method (AMVn Automated Micro Viscometer). The surface tension was measured using the hanging droplet method (Kruis Easydrop). Atomic force microscopy (AFM) was used to measure the surface topography (Veeco Dimension 3100 Scanning Probe Microscope), using Si probes in tapping mode.

RESULTS AND DISCUSSION

Inkjet printing of high-conducting PEDOT:PSS

For future roll-to-roll production of OPVs, ITO-free transparent electrodes need to be implemented. We have previously published the use of Ag-grids/PEDOT:PSS electrodes for OPV and organic light-emitting diode (OLED) applications.[11,17,18] The deposition by inkjet printing of the PEDOT:PSS layer has shown to be advantageous as it allows direct patterning of the electrode and avoids post-patterning steps. In the first part of this article, we will focus on the wetting behavior and layer formation of high-conducting PEDOT:PSS onto SiN_x and Ag.

The layer formation of inkjet-printed PEDOT:PSS on top of an Ag grid is influenced by the grid topology, but it is also affected by the chemical heterogeneity of the substrate. A substrate with alternating SiN_x and Ag bars was prepared by printing Ag stripes onto a glass/SiN_x substrate. After an N_2 plasma treatment, the surface energy difference between the materials was reduced and closed layers were obtained.[15] A test pattern of PEDOT:PSS lines with varying line widths was printed, as is shown in Figure 2. For a good functioning electrode, a homogeneous layer of PEDOT:PSS covering the Ag grid is essential. However, as can be seen for example in the red encircled area, the PEDOT:PSS line becomes wider on SiN_x as compared to Ag. This indicates a flow of ink from the Ag surface onto the SiN_x, which may lead to local depletion

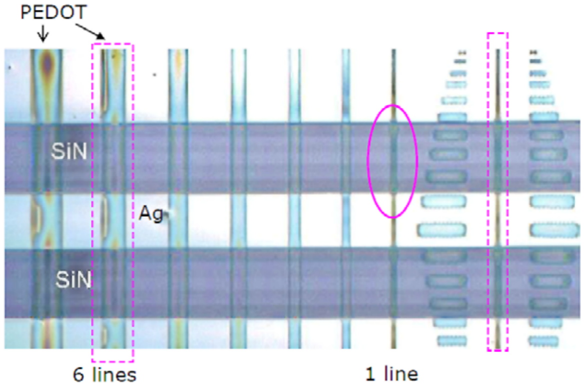

Figure 2. Inkjet-printed PEDOT:PSS (vertical lines, single line width = 100 μm) on a substrate with alternating SiN_x and Ag lines (horizontal lines).

of PEDOT:PSS. This is related to the difference in surface energy of the two substrate materials. Actually, the applied silver Cabot ink has a slightly higher disperse surface energy (35–40 mN/m) than SiN_x (30–35 mN/m), while the polar surface energy is lower (7–15 mN/m versus 17–25 mN/m). Furthermore, the topology and the capillary flow also cause PEDOT:PSS to flow towards the SiN_x surface.

To incorporate inkjet-printed PEDOT:PSS into devices, closed layers with a smooth surface are desired. The height variations need to be limited such that the subsequent layer printed on top can cover the topology completely and short cuts are prevented. For OLED applications, height variations leading to variations in layer thicknesses will also appear as light intensity variations. However, for OPVs, a photoactive layer of at least 200 nm will be printed on top. While variations in layer thickness may locally affect the efficiency, the requirements on layer smoothness are less stringent than for OLEDs. Here, the surface roughness of inkjet-printed high-conducting PEDOT:PSS was evaluated with AFM. Figure 3 shows the AFM micrograph and a corresponding height profile. Here, it can be seen that height variations occur in the order of 10–30 nm. For application in OPVs, this is well within the acceptable range.

Inkjet printing of P3HT/PCBM

Bulk heterojunction photoactive layers have been applied by roll-to-roll compatible techniques most often using chlorinated aromatic solvents. However, this is undesirable due to environmental and health risks. Therefore, in this study, we have formulated an ink using only non-chlorinated solvents. This task is complicated by the many requirements for an inkjet-printable ink, limited polymer solubility, and the sensitivity of the bulk heterojunction morphology to processing parameters such as the solvent and drying and thermal annealing procedures. To be suitable for inkjet printing, the ink should have sufficient viscosity (2–20 mPa s), a low surface tension (25–35 mN/m), and a boiling point in the range 130–200°C. Logically, the polymer and PCBM should have sufficient solubility to limit the amount of liquid that has to be deposited to achieve the desired film thickness of ∼200 nm. For large-scale applications, the ink should be stable for longer periods of time, so as to prevent nozzle clogging. Prediction of phase separation of P3HT/PCBM heterojunctions as a function of the mentioned processing parameters, and consequently the expected cell performance, is not straightforward. Therefore, we use the inkjet ink requirements as a starting point for the development of a new ink formulation, while the solubility of the photoactive layer components is tested for concentrations up to 2 wt%.

A first candidate to replace chlorobenzene as solvent for P3HT/PCBM is o-xylene, as many of its physical properties are similar to those of chlorobenzene; see Table I. 1 wt% P3HT/1 wt% PCBM was dissolved by heating at 70°C overnight. However, upon cooling to room temperature, aggregation and gelation were observed, indicating the limited solubility of P3HT and PCBM in o-xylene. A 0.8 wt% polymer solution was stable upon cooling towards gelation and aggregation, as after 30 min at room temperature no significant increase in viscosity was measured. However, as listed in Table I, the solution had a viscosity of 0.85 mPa s, which is below the range indicated to be applicable for inkjet printing. Inks with varying viscosities were formulated, with a highest viscosity of 1.7 mPa s, just below the inkjet print range. However, stable jetting over the printing period was still achieved. Ink D was stable up to a month of shelf time, while ink C showed gelation already after a week of shelf time.

As was the case for the PEDOT:PSS ink, the layer formation and the wetting behavior of the photoactive layer ink onto the substrate are of paramount importance. The photoactive layer is printed on top of the PEDOT:PSS layer, a relatively polar surface. Figure 4 shows 3 cm by 3 cm layers of P3HT/PCBM printed using inks A–D onto high-conducting PEDOT:PSS. Fig. 4d shows severe dewetting of the ink. This might be related to the relatively high surface tension of the ink. However, all inks have surface tensions in a similar region, although variations in the disperse and polar parts may explain the observed differences. Inks A and B show poor pinning. This could be resolved using a higher solids content; however, this is not possible due to the low solubility and negative effect on ink stability. Ink B already shows improved pinning compared to ink A, but the best layer was obtained using ink C. This shows that ink formulation is a matter of finding the delicate balance between good ink properties and wetting behavior. In this case, based on the ink properties listed in Table I, ink A seemed the best candidate, while ink D was the most stable. However, the less stable ink C with lower viscosity shows significantly better layer formation.

Device performance

By inkjet printing, closed PEDOT:PSS and P3HT/PCBM layers were obtained. To demonstrate the feasibility for roll-to-roll manufacturing of inkjet printing, the performances of devices with direct cell configurations with inkjet-printed layers were compared to that of a reference device that was produced by spin coating. Figure 5 shows a photograph of a device with two inkjet-printed layers: high-conducting PEDOT:PSS and P3HT/PCBM. Here, already an advantage

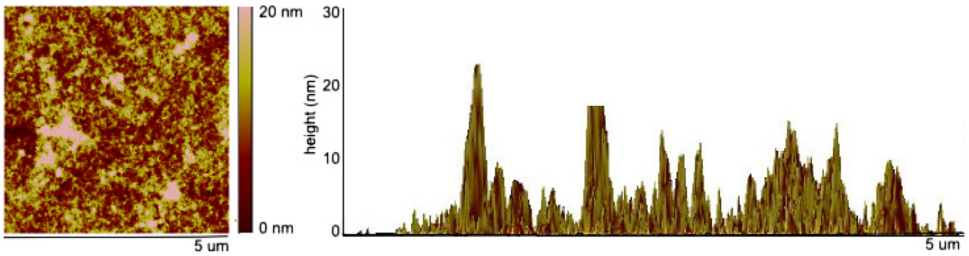

Figure 3. AFM micrograph and height profile of inkjet-printed high-conducting PEDOT:PSS.

Table I. Solvent and ink properties.

Solvent	Vapor pressure [mm Hg]	Boiling point [°C]	Surface tension [mN/m]	Viscosity [mPa s]
Chlorobenzene	11.80 (25°C)	132	33.0	0.80 (20°C)
o-Xylene	5.10 (20°C)	144	28.7	0.76 (25°C)
P3HT/PCBM (0.8 wt%/0.8 wt%)				
o-Xylene			28.4	0.85
Ink A			30.9	1.70
Ink B			32.2	1.56
Ink C			32.4	1.31
Ink D			30.3	1.35

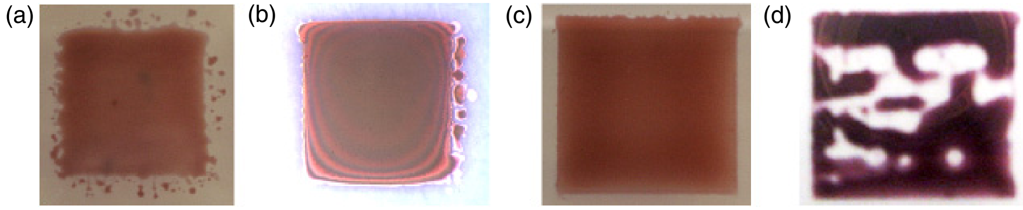

Figure 4. P3HT/PCBM layers inkjet printed onto PEDOT:PSS using inks A, B, C and D, respectively. All printed areas are 3 cm by 3 cm.

of inkjet printing over slot-die coating or other large-area deposition techniques is apparent. Due to the high conductivity of the adjusted PEDOT:PSS formulation, the active areas cannot be connected by a single layer. The PEDOT:PSS is therefore only printed to cover the ITO-electrode area. For future roll-to-roll manufacturing, this will make an additional processing step to locally remove the PEDOT:PSS layer superfluous. The photoactive layer is printed on top over an area of 2 cm by 2 cm, and the devices were finished by evaporating an LiF/Al cathode.

The performance of the inkjet-printed device was compared to that of a spin-coated device using chlorobenzene as solvent for P3HT/PCBM, currently the solvent leading to the best performing devices. Comparable performance was observed for the inkjet-printed device using non-chlorinated solvents (ink C) and the spin-coated reference, and the I–V-characteristics measured under illumination and in the dark are shown in Fig. 5. The inkjet-printed cell reached 2.4% at the maximum power point (MPP), while for the spin-coated reference device an MPP of 2.7% was measured. The V_{OC} of both cells was 0.54 V, a typical value for devices with P3HT/PCBM bulk heterojunction layers. While the I_{SC} was comparable, the fill factor was lower for the inkjet-printed cell (45% versus 54%). Notably, the inkjet-printed cell showed little or no leakage current in the dark current. This is likely related to the patterning of the high-conductive PEDOT:PSS.

CONCLUSIONS AND OUTLOOK

The full solution-processed roll-to-roll production of stable OPVs with high conversion efficiency is a process requiring a significant amount of fundamental and technological knowledge. In this article we have described another step forward by demonstrating an OPV device with two inkjet-printed layers with similar performance to that of a spin-coated reference device using chlorobenzene. For the inkjet-printed photoactive layer, we were able to formulate an ink free of halogenated solvents, by testing solubility, ink stability and rheological properties. Eventually, the layer formation of the photoactive material on PEDOT:PSS predominated the ink formulation process. To render the cell compatible with ITO-free substrates, inkjet-printed high-conducting PEDOT:PSS was used as a hole-collecting layer. It showed different wetting behavior on SiN_x and Ag surfaces leading to

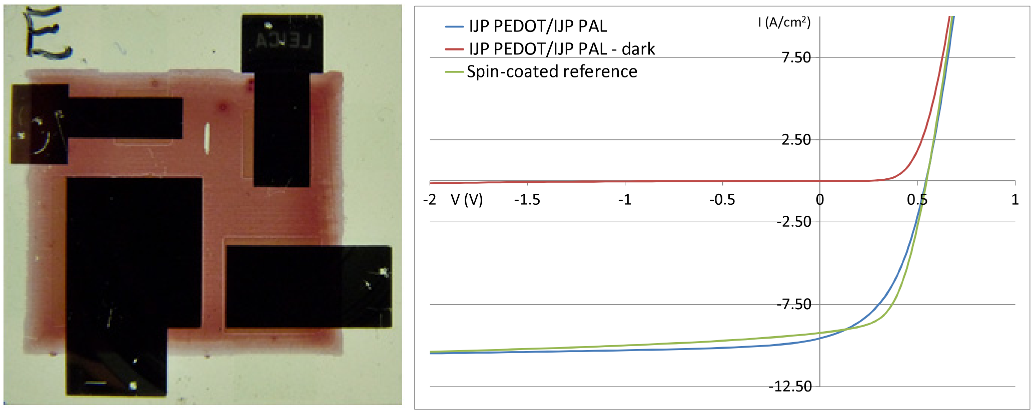

Figure 5. Photograph showing a 3 cm by 3 cm device with inkjet-printed PEDOT:PSS and P3HT/PCBM layers, together with *I*–*V*-curves of the inkjet-printed and spin-coated reference device.

layer inhomogeneity; however, a smooth PEDOT:PSS layer was obtained by applying a plasma to the substrate surface. We envision that inkjet-printed layers as described in this article can be incorporated with earlier published processes into all solution-processed OPV devices on flexible foils.

ACKNOWLEDGMENTS

The Holst Centre is an open innovation research centre founded by TNO and IMEC that is developing roll-to-roll production techniques for foil-based organic electronics and wireless autonomous transducer solutions, in corporation with industry and universities. This research has been funded by the Dutch Ministry of Economic Affairs, Philips Research, Merck KGaA, and Agfa-Gevaert. The authors would like to thank Yulia Galagan and Mathieu Foucaud for their help in the preparation and measurement of devices.

REFERENCES

[1] P. Kumar and S. Chand, Prog. Photovolt: Res. Appl. **20**, 377–415 (2012).
[2] G. Li and Y. Yang, Nat. Photon. **6**, 153–161 (2012).
[3] C. J. Brabec, Sol Energ. Mat. Sol. Cell. **83**, 273–292 (2004).
[4] Y. Galagan, A. de Vries, R. Langen, W. Andriessen, S. Verhees, and Veenstra J. Kroon, Chem. Eng. Process. **50**, 454–461 (2011).
[5] F. C. Krebs, M. Jorgensen, K. Norman, O. Hageman, J. Alstrup, T. D. Nielsen, J. Feynbo, K. Larsen, and J. Kristensen, Sol. Energ. Mat. Sol. Cell. **93**, 422–441 (2009).
[6] M. Singh, H. M. Haverinen, P. Dhagat, and G. E. Jabbour, Adv. Mater. **22**, 673 (2010).
[7] E. Tekin, P. J. Smith, and U. S. Schubert, Soft. Matter **4**, 703–713 (2008).
[8] S. H. Eom, S. Senthilarasu, P. Uthirakumar, S. C. Yoon, J. Lim, C. Lee, H. S. Lim, J. Lee, and S. Lee, Org. Electron. **10**, 536–542 (2009).
[9] C. N. Hoth, S. A. Choulis, P. Schilinsky, and C. J. Brabec, Adv. Mater. **19**, 3973–3978 (2007).
[10] F. C. Krebs, Sol. Energ. Mat. Sol. Cell. **93**, 1636–1641 (2009).
[11] Y. Galagan, E. W. C. Coenen, S. Sabik, H. Gorter, M. Barink, S. C. Veenstra, J. M. Kroon, R. Andriessen, and P. W. M. Blom, Sol. Energ. Mat. Sol. Cell. **104**, 32–38 (2012).
[12] E. Rubingh, P. Kruijt, and R. Andriessen, *Proc. LOPE-C*, (2009).
[13] F. Padinger, R. S. Rittberger, and N. S. Sariciftci, Adv. Funct. Mater. **13**, 85–88 (2003).
[14] T. Aernouts, G. Aleksandrov, C. Girotto, J. Genoe, and J. Poortmans, Appl. Phys. Lett. **92**, 033306 (2008).
[15] S. H. Eom, H. Park, S. H. Mujawar, S. C. Yoon, S. Kim, S. Na, S. Kang, D. Khim, D. Kim, and S. Lee, Org. Electron. **11**, 1516–1522 (2010).
[16] C. N. Hoth, P. Schilinsky, S. A. Choulis, and C. J. Brabec, Nano Lett. **8**, 2806–2813 (2008).
[17] M. Ren, H. Gorter, J. Michels, and R. Andriessen, J. Imaging Sci. Technol. **55**, 040301-1–040301-6 (2011).
[18] Y. Galagan, B. Zimmerman, E. W. C. Coenen, M. Jorgensen, D. M. Tanenbaum, F. C. Krebs, H. Gorter, S. Sabik, L. H. Slooff, S. C. Veenstra, J. M. Kroon, and R. Andriessen, Adv. Energy Mater. **2**, 103–110 (2001).